Synthesis and Evaluation of Glycopolymeric Decorated Gold Nanoparticles Functionalized with Gold–Triphenyl Phosphine as Anti-Cancer Agents

ARTICLE *in* BIOMACROMOLECULES · AUGUST 2014

Impact Factor: 5.75 · DOI: 10.1021/bm5010977 · Source: PubMed

6 AUTHORS, INCLUDING:

Christian KWEKU Adokoh
University of Cape Coast
19 PUBLICATIONS **72** CITATIONS
SEE PROFILE

Mary Hitt
University of Alberta
66 PUBLICATIONS **2,897** CITATIONS
SEE PROFILE

James Darkwa
University of Johannesburg
159 PUBLICATIONS **1,382** CITATIONS
SEE PROFILE

Ravin Narain
University of Alberta
98 PUBLICATIONS **2,274** CITATIONS
SEE PROFILE

Article

pubs.acs.org/Biomac

Synthesis and Evaluation of Glycopolymeric Decorated Gold Nanoparticles Functionalized with Gold-Triphenyl Phosphine as Anti-Cancer Agents

Christian K. Adokoh,[†,‡] Stephen Quan,[†] Mary Hitt,[§] James Darkwa,[‡] Piyush Kumar,[§] and Ravin Narain*[,†]

[†]Department of Chemical and Materials Engineering and [§]Department of Oncology, Faculty of Medicine and Dentistry, University of Alberta, Edmonton, AB, Canada

[‡]Department of Chemistry, University of Johannesburg, P.O. Box 524, Auckland Park 2006, South Africa

Supporting Information

ABSTRACT: In this study, statistical glyco-dithiocarbamate (DTC) copolymers were synthesized by reversible addition−fragmentation chain transfer polymerization (RAFT) and subsequently used to prepare glyconanoparticles and conjugated glyconanoparticles with the anticancer drug, gold(I) triphenylphosphine. These glyconanoparticles and the corresponding conjugates were then tested for their in vitro cytotoxicity in both normal and cancer cell lines using Neutral Red assay. The glyconanoparticles and their Au(I)PPh_3 conjugates were all active against MCF7 and HepG2 cells, but galactose-functionalized glyconanoparticles {P(GMA-EDAdtc($AuPPh_3$)-st-LAEMA)AuNP} were found to be the most cytotoxic to HepG2 cells (IC_{50} ∼ 4.13 ± 0.73 μg/mL). The p(GMA-EDAdtc($AuPPh_3$)-st-LAEMA)AuNP was found to be a 4-fold more potent antitumor agent in HepG2 cells, and the overexpressed asialoglycoprotein (ASGPR) receptors revealed to play an important role in the cytotoxicity, presumably by the enhanced uptake. In addition, the glyconanoparticles Au(I) conjugates are found to be significantly more toxic as compared to the standard chemotherapeutic reagents such as cisplatin and cytarabine.

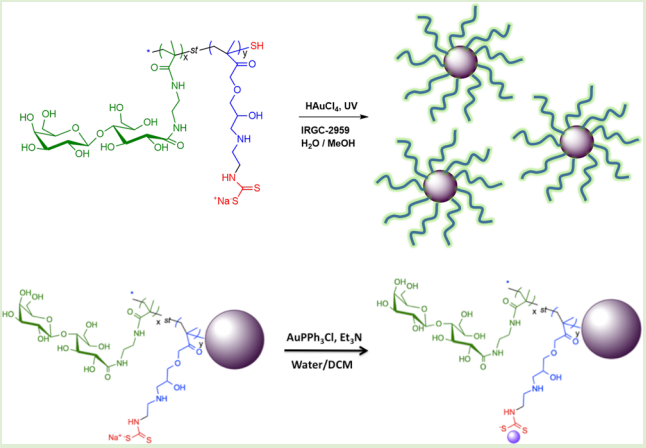

INTRODUCTION

Over the past decade, platinum-based anticancer therapeutics such as cisplatin, carboplatin, and oxaliplatin, have successfully demonstrated profound effects on regressing rapidly proliferating cancers, improving efficacy of palliative treatment and increasing overall survival rate of the patients.[1−3] However, high systemic toxicity, undesirable side effects, and relatively low tumor specificity associated with these platinum-based drugs underscores the need for the development and optimization of other metal-based anticancer agents.[4,5] The use of gold compounds as therapeutics, also known as chrysotherapy, has been recognized as one of the oldest forms of medicinal treatment of physiological ailments, such as rheumatoid arthritis and psoriasis, due to its unique anti-inflammatory properties.[6] Interestingly, engineered gold nanoparticles (AuNP) display an extraordinary combination of chemical inertness, surface modifiable substrate, and size/shape-dependent optical properties, which makes them ideal candidates in biomedical applications.[7,8] Carbohydrate-based anticancer agents have been explored with the aim of increasing the efficacy and decreasing the side effects of traditional anticancer Pt-based drugs.[9,10]

Recently, polymeric systems have been recognized as playing an important role in drug and gene delivery for cancer therapy.[11−13] Glycopolymers continue to gain significant recognition due to the multivalency and tumor-targeting properties. Functionalized AuNPs with nontoxic polymers have properties that can be exploited in receptor-mediated tumor cell targeting, enhanced biocompatibility, and biorecognition.[14−17] The synthesis of statistical and block copolymers via Reversible Addition−Fragmentation Chain Transfer (RAFT) polymerization has been extensively explored and implemented in developing novel cancer theranostics.[18−20] Polymer chains with pendant thiol substituent's play a crucial role in offering the well-known covalent interaction between sulfur−Au complexes leading to the formation of AuNPs.[21] Additionally, incorporating carbohydrates into polymer chains have been intensively studied in cell−cell communication, delivery vectors, and targeted cell surface receptor binding interactions, making them logical candidates for drug delivery

Received: July 27, 2014
Revised: August 22, 2014
Published: August 27, 2014

dx.doi.org/10.1021/bm5010977 | Biomacromolecules 2014, 15, 3802−3810

Scheme 1. Synthesis of Statistical Dithiocarbamate Copolymer p(GMA-EDAdtc-st-LAEMA)

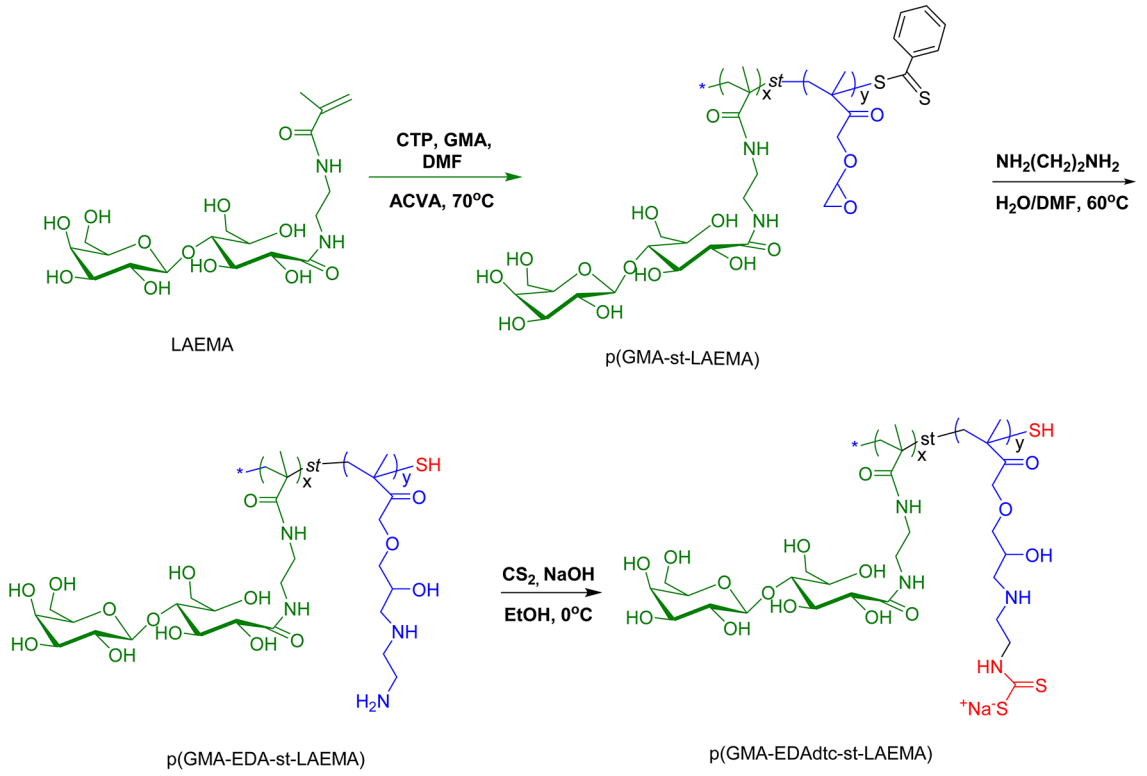

applications.[22] More specifically, galactose sugar molecules have been explored in targeting the asialoglycoprotein receptor (ASGPR) overexpressed in hepatocellular carcinomas (HCC) by carbohydrate−protein interactions.[23,24] Narain and co-workers recently reported that, glycopolymer-based gold(I) phosphines DTC-conjugates displayed higher accumulation and cytotoxicity in cancer cells under hypoxic conditions in comparison to the normoxic conditions.[20] It was noted that the glycopolymer gold(I) conjugates showed a significantly higher degree of inhibition of cell proliferation and its activity efficiency was dependent on the solubility and low molecular weight of the copolymers. Further improvement in solubility and transfection efficiency of the glycopolymer derivatives will benefit in the construction of better drug-delivery systems. The presence of the carbohydrate moieties on the nanoparticle surface has proven to have a drastic effect on the bimolecular events. Certain carbohydrate moieties, such as galactose residues, exhibit high recognition toward hepatocytes.[25] Those specific carbohydrate residues can be easily attached to the nanoparticle surface for targeted delivery. Furthermore, highly monodisperse and multivalent gold glyconanoparticles showed promise as highly stable and biocompatible materials that can be easily synthesized in an aqueous environment. In addition to nanoparticle size,[26,27] nanoparticle composition (i.e., surface chemistry and polymer architecture) plays a critical role in cell uptake and is of upmost importance in immune activation and modulation.[28] Several biospecific recognition molecules such as antibodies, DNA probe molecules, biotin and streptavidin, or enzymes have been conjugated to nanoparticles for various biological applications.[29−32] Narain et al. have reported several glycopolymer gold nanoparticles, their complexation with DNA, cellular uptake, and transfection efficiencies.[33−36] Although various macromolecules stabilized gold nanoparticles have been synthesized and their biological and chemical properties are reported,[37−41] no previous studies on direct conjugation of toxic cancer drugs onto glycopolymer gold nanoparticles and their biological properties has been reported so far. In our endeavor to improve the efficiency of the previously reported glycopolymer gold(I) conjugate,[20] we effectively designed polymeric dithiocarbamate galactose gold nanoparticles gold(I) conjugate as an anticancer agent. This is the first study of glyconanoparticles conjugated to gold(I) triphenyl phosphine as an anticancer agent.

The use of RAFT polymers as delivery vehicle has been limited[42] due to acute toxicity[43] caused by the degree of hydrolysis of macro chain transfer agent (CTAs) of the free thioether end groups in living tissues interacting with a variety of proteins. However, end group modification of RAFT based polymers has been described as a possible approach before their use for systemic applications.[44] In view of this, our approach of using ethanolamine (EA) functionalized poly(glycidyl methacrylate) (PGMA) vectors, as reported by Pun and co-workers,[45] as a co-monomer was crucial, since it introduces an end group modification of the macro chain transfer agent and at the same time introducing a thiol end moiety for further functionalization. Ethanolamine (EA) functionalized poly(glycidyl methacrylate) (PGMA) vectors have been reported to produce good transfection efficiency while exhibiting very low toxicity.[45,46]

This study focuses on the potential anticancer activity of triphenylphosphine gold(I) complexes conjugated with well-defined hydrophilic copolymers using dithiocarbamate as a stabilizing ligand. In fact, phosphinogold(I) DTC on its own is a good anticancer agent, so attaching this unit to polymeric gold nanoparticles allows the polymeric gold particles to be used as an efficient drug delivery vehicle.[47] In our expedition to improve biological efficacy of the gold(I) conjugate, we report here a careful conjugation of gold(I) triphenyl phosphine onto

dx.doi.org/10.1021/bm5010977 | Biomacromolecules 2014, 15, 3802−3810

glyconanoparticles and to test the hypothesis that combining glycopolymer dithiocarbamate gold nanoparticles and gold(I) triphenyl phosphine can lead to a new class of gold-based anticancer drugs. Since copolymers with statistical architectures are ideal for the desired biological features,[9,33,34,48,49] we synthesized statistical glycopolymers decorated with dithiocarbamate using glycomonomers 2-gluconamidoethyl methacrylamide (GAEMA), 2-lactobianamidoethyl methacrylamide (LAEMA), and glycidylmethacrylamide (GMA) of varying molecular weights. Herein, we propose engineered glycopolymer surface-functionalized gold nanoparticles conjugated with gold(I) triphenylphosphine, which can specifically target ASGPR overexpressing HCC by exploiting the glucose-derived and galactose moieties on the surface for targeting ASGP receptors overexpressed on the liver cancer cellular surface. Glyco-dithiocarbamate (DTC) statistical polymers are prepared via RAFT polymerization to incorporate the desired backbone chemistry. The synthesized galactose-based P(GMA-EDAdtc-($AuPPh_3$)-st-LAEMA)-AuNP were found to be a 4-fold more potent anticancer agent (IC_{50} = 4.13 ± 0.73 μg/mL) in HepG2 cells as compared to the corresponding glucose derivative in ASGPR-deficient HeLa cells and significantly more toxic compared to standard chemotherapeutic reagents cisplatin and cytarabine.

MATERIALS AND METHODS

Materials. All the chemicals and cell culture products were purchased from Sigma-Aldrich and were used without purification. Glycidyl methacrylate (GMA, 97%, Aldrich) was purified by column chromatography using alumina prior to its use. 4,4-Azobis(4-cyanovaleric acid) (ACVA) was purchased from Acros Organics and used as received. 4-Cyanopentanoic acid dithiobenzoate (CTP; Scheme 1), carbon disulfide, ethylene diamine (EDA), tetrahydrothiophene, hydrogen tetrachloroaurate, and triphenyl phosphine were purchased from Sigma-Aldrich, Canada. All solvents were purchased from Caledon Laboratories and used without any further purification. Monomers, 2-gluconamidoethyl methacrylamide hydrochloride (GAEMA) and 2-lactobionamidoethyl methacrylamide (LAEMA), were prepared in-house according to previously reported procedures.[50−53]

Methods. *Polymer Characterization.* ^{1}H NMR spectra of the monomers and polymers were recorded using a Varian spectrometer (500 MHz) to confirm and determine the chemical structures of the synthesized polymers. Molecular weight and molecular weight distributions were determined by conventional Viscotek gel permeation chromatography (GPC) system using aqueous eluents, two Waters WAT011545 columns at room temperature and a flow rate of 1.0 mL/min using a 0.5 M sodium acetate/0.5 M acetic acid buffer as eluent. Statistical polymers, P(GMA-st-LAEMA), P(GMA-st-GAEMA), and P(GMA-EDA-st-GAEMA), were characterized based on seven near-monodisperse Pullulan standards (M_w 5900−404000 g mol^{-1}).

Fourier Transform Infrared (FT-IR). FT-IR spectral analyses using KBr pellets of the synthesized samples were carried out on a Nicolet 8700 (Thermo) instrument and the diffuse reflectance spectra were scanned over a range of 4000−400 cm^{-1} wave numbers.

Dynamic Light Scattering (DLS). DLS measurements were performed with a ZetaPlus-Zeta Potential Analyzer (Brookhaven Instruments Corporation) at a scattering angle $\theta = 90°$. p(GMA-EDA-st-LAEMA)-stabilized gold nanoparticles solutions were filtered through Millipore membranes (0.45 μm pore size). The data were recorded with Omni size software.

UV−Visible Spectroscopy. UV−visible absorption spectra (400−800 nm) were recorded on a Cary UV 100 spectrophotometer from the aqueous solutions of polymeric AuNPs at room temperature.

Synthesis of Glyco Decorated Dithiocarbamate Statistical Polymers. RAFT statistical copolymers of glycidyl methacrylamide (GMA) and 2-gluconamidoethyl methacrylamide, P(GMA-st-GAEMA), glycidyl methacrylamide and 2-lactobionamidoethyl methacrylamide P(GMA-st-LAEMA) were synthesized. The RAFT polymerization was achieved at 80 °C, employing ACVA as the initiator and CTP as the chain transfer agent, according to previously reported procedures[15,34,35] using the following reagents.

P(GMA-st-GAEMA): GMA (0.166 g, 1.17 × 10^{-3} mol) and GAEMA (1.07 g, 3.5 × 10^{-3} mol) in water (5 mL), and ACVA (3.5 mg, 0.0125 × mmol) and 4-cyanopentanoic acid dithiobenzoate (CTP; 17.4 mg, 1.17 mmol) in 2 mL of 1,4-dioxane. ^{1}H NMR (500 MHz, D_2O) δ_H 4.75 (s, 1H), 4.35 (s, 1H), 4.12 (s, 1H), 4.03 (s, 1H), 3.84 (d, 1H), 3.78 (s, 2H), 3.69 (s, 1H), 3.36 (d, 3H), 1.86 (s, br, 2H), 1.09−0.93 (d, br, 3H).

P(GMA-st-LAEMA): LAEMA (1.00 g, 2.04 × 10^{-3} mol), GMA (0.17 g, 1.17 × 10^{-3} mol), ACVA (3.5 mg, 0.0125 mmol), and 4-cyanopentanoic acid dithiobenzoate (CTP; 17.8 mg, 0.062 mmol) in *N*,*N*′-dimethylformamide (DMF; 2 mL). ^{1}H NMR (500 MHz, D_2O) δ_H 4.74 (s, 1H), 4.58 (s, br, 1H), 4.42 (s, 1H), 4.21 (s, 2H), 4.09 (s, 1H), 4.01 (s, 2H), 3.94 (s, 2H), 3.87 (s, 1H), 3.78 (s, br, 4H), 3.67 (s, 1H), 3.58 (s, 1H), 3.36 (s, br, 2H), 1.96 (s, 2H), 1.09−0.92 (m, 3H).

Decoration of Statistical Copolymers by Ethylenediamine (EDA). Statistical copolymers of p(GMA-st-LAEMA) and p(GMA-st-GAEMA) were decorated by the optimized EDA in a 30-fold molar excess.[27] In a typical procedure, EDA (2.0 mL, 10.5 mmol) was dissolved in anhydrous DMF (10 mL) in a 25 mL round-bottom flask equipped with a magnetic stirring bar, and respective polymers (50 mg) in 2 mL of DMF were added dropwise. After reaction at 60 °C for 7 h, the mixture was purified by dialysis (pore size 12 kDa cutting molecular weight) against 4 L of distilled water, which was replaced three times per day over the course of 3 days. Finally, the amine-decorated polymers were collected by freeze-drying for further characterization.

p(GMA-EDA)-st-p(LAEMA): ^{1}H NMR (500 MHz, D_2O) δ_H 4.12−3.80 (m, 3H), 3.81 (m, 1H), 3.86 (s, br, 1H), 3.57 (s, 1H), 3.48 (s, br, 3H), 2.79 (s, br, 5H), 1.95−1.75 (m, 4H), 1.15 (s, 3H), 0.91 (s, 3H). IR (diamond, ATR, cm^{-1}): 3350 υ(OH), 2840 υ(CH_2), 966 υ(C−S), 1639 υ(C═O), 1530 υ(N−C).

p(GMA-EDA)-st-p(GAEMA): 0.12 g (40%) ^{1}H NMR (500 MHz, D_2O) δ_H 4.16 (s, br, 1H), 3.99 (s, br, 2H), 3.83−3.65 (m, 4H), 3.24 (s, 2H), 3.24 (s, 2H), 2.97−2.82 (m, 6H), 1.84 (s, br, 6H), 1.33 (s, br, 3H), 1.11 (s, br, 3H), 0.94 (s, br, 3H).

Synthesis of Polymeric DTC Compounds. The DTCs compounds were synthesized with slight modifications to a previously reported method.[20] All values are based on the amount of the PGMA in the polymer. EDA decorated polymers (100 mg) were dissolved in 0.25 M NaOH ethanolic solution (8 mL) at 0 °C, after which carbon disulfide (0.04 mL, 0.71 mmol) in ethanol (2 mL) was added in drops. The reaction was stirred for 24 h, and the pale yellow solid, so obtained, was filtered, washed with ethanol to remove excess starting materials, and dried under vacuum to afford a degree of colored solid, depending on monomer and molecular weight targeted.

p(GMA-EDAdtc)-st-p(LAEMA) (LPdtc): ^{1}H NMR (D_2O) δ_H 4.11 (s, br, 1H), 4.02 (s, br, 3H), 3.67−3.64 (m, 6H), 3.37 (s, br, 4H), 2.72 (s, 1H), 1.83 (s, br, 4H), 1.78 (s, br, 4H, $2CH_2$), 1.34 (s, br, 3H), 1.00 (s, br, 3H, CH_3). IR (diamond, ATR, cm^{-1}): 989 υ(C−S), 1050 υ(C═S), 1453 υ(N−C).

p(GMA-EDAdtc)-st-p(GAEMA) (GPdtc): ^{1}H NMR (D_2O) δ_H 4.16 (s, 1H), 4.09 (s, 1H), 4.00 (s, br, 2H), 3.75−3.63 (m, 5H), 3.34 (s, br, 2H), 3.24 (s, br, 1H), 2.77 (s, br, 2H), 1.75 (s, br, 7H), 1.33 (s, br, 4H), 1.11 (s, br, 3H, CH_3), 0.96 (s, br, 3H, CH_3). IR (diamond, ATR): 987 υ(C−S), 1050 υ(C═S), 1463 υ(N−C).

Synthesis of Statistical Glucose-Derived and Galactose Copolymer-Coated Au Nanoparticles in the Presence of Irgacure-2959 (IRGC). The glyco-dithiocarbamate polymer-coated gold nanoparticles were synthesized via photo irradiation using Irgacure-2959 (IRGC) as a photoinitiator. The molar ratios of $HAuCl_4$/IRGC in double-distilled water was 1:3 as polymer concentration was varied. In a typical synthesis, 1, 2, and 5 mg each of polymers, LPdtc (ca. 22 kDa) and GPdtc (ca. 20 kDa) were dissolved in deionized water (15 mL), and the solution was added to

$HAuCl_4$ (0.005 mg/mL) solution in double-distilled water (5 mL). A methanolic solution of Irgacure-2959 (8.5 mg, 0.038 mmol) initiator (5 mL) was then added to $HAuCl_4$ and polymer mixture and degassed for 15 min, after which irradiation was done for 15 min. The photo irradiation of the reaction mixture was carried out using 16, 12, 8, and 4 75 W UV lamps at a wavelength of 300 nm in a Rayonet photo reactor (Southern N.E. Ultraviolet Co.). After 15 min, the reaction mixture was taken off the photo reactor and stirred at room temperature for 5 min. The gold nanoparticles produced were filtered through Millipore membranes (0.45 μm pore size) and centrifuged at 20000 rpm for 2 h to remove excess polymer. The pellet was resuspended in deionized water. Three forms of polymer concentrations (1, 2, and 5 mg) were synthesized to study concentration variation effect.

Synthesis of Statistical Copolymer AuNP-Decorated Gold(I) Triphenylphosphine Complex. The title complex was synthesized according to literature procedure[15] with slight modification. A solution of $[AuCl(PPh_3)]$ (2 mg, 0.004 mmol) and triethylamine (8.5 μL) in dichloromethane (5 mL) was added to a solution of respective polymeric modified galactose dithiocarbamate stabilized AuNPs (6 mL; ca. 53.5 nM) under nitrogen. The resulting solution was stirred for 3 h. The aqueous layer was separated and centrifuged three times to remove unwanted materials, after which the pellet was resuspended in water for further characterization.

Determination of pH. Basic-20 pH meter was calibrated using buffer solutions of pH 4.0, 7.0, and 10.0. Polymeric AuNPs pH was adjusted from 2 to 12 by a margin of 2 through the addition of 0.1 M NaOH and 0.1 M HCl solutions. After the desired pH was obtained, the electrode was dipped in the analyte solution to read the pH values. The electrode was rinsed with double-distilled water after every successive measurement.

Critical Flocculation Concentration (CFC). The filtered glyco-stabilized gold nanoparticles were centrifuged at 15000 rpm for 90 min at room temperature. The modified particles were then resuspended in phosphate buffer solution. The centrifugation step was repeated three times to ensure complete removal of free ligands. The approximate glyco-stabilized gold nanoparticles concentration of about 53.4 nM (3 mL) was used for the Critical Flocculation Concentration (CFC) test. After each 5 min, 500 μL of phosphate buffer, as well as 10, 100, and 200 μL of 10% NaCl (1.7 M) solutions, was added to each solution and allowed to stand for 1 h. Then the CFC tests were done by UV−vis measurement in the wavelength range of 300−800 nm.

Cell Culture. HepG2 hepatocellular carcinoma, MCF-7 breast cancer, WI38 lung fibroblast, and HeLa cervical carcinoma cell lines were incubated in low-glucose DMEM medium supplemented with 10% fetal bovine serum (FBS), 2 mM glutamine, and 1× antibiotic-antimycotic (100 units of penicillin, 100 μg streptomycin, 0.0085% fungizone) in a humidified atmosphere at 37 °C and 5% CO_2. At about 80% confluency, the cells were subcultured by dissociating with 0.25% trypsin in versene twice per week. All tissue culture reagents were purchased from Gibco.

Determination of IC_{50} Values. HepG2, MCF-7, HeLa, and WI38 (10000 cells/well) were seeded into 96-well tissue culture plates in triplicate and were allowed to adhere overnight. The medium was removed and replaced with fresh DMEM medium containing 5% FBS with varying concentrations (0.1 to 0.001 mg/mL) of glycopolymer-AuNP-$AuPPh_3$, and the cells were incubated for 24 h with drugs under evaluation. The cell viability was determined by Neutral Red assay. Briefly, 0.1 mL of 0.04 mg/mL Neutral Red solution was added to each well and cells were incubated for 4 h, followed by the addition of 50% methanol/49% deionized H_2O/1% acetic acid destain solution. The 96-well tissue culture microplates were shaken for 15 min and the fluorescence was read at 540 nm using FLUOstar Omega microplate reader. The IC_{50} values were calculated by sigmoidal curve fitting on Boltzmann distribution function using Origin 9.1 Pro graphing software.

Competition Binding Assay with ASGPR Cell Surface Receptors. HepG2 and MCF-7 (10000 cells/well) were seeded into 96-well tissue culture plates in triplicates and were allowed to adhere overnight. The medium was removed and replaced with DMEM medium containing 5% FBS with the competitors asialofetuin and P(GMA-EDAdtc-st-LAEMA) polymer at 10× the concentration of drug being evaluated (100 μL of 10 μg/mL of P(GMA-EDAdtc($AuPPh_3$)-st-LAEMA)AuNP). In another experiment, the cells were pretreated with asialofetuin at 10× concentration of drug for 2 h in DMEM medium before the addition of P(GMA-EDAdtc($AuPPh_3$)-st-LAEMA)AuNP to the 96-well tissue culture plate. The polymer and drug compound were incubated with cells for 24 h, and the cell viability was determined by Neutral Red assay, as described above, measured using FLUOstar Omega microplate reader.

RESULTS AND DISCUSSION

Statistical glyco-glycidyldithiocarbamate polymers, p(GMA-EDAdtc-st-GAEMA) and p(GMA-EDAdtc-st-LAEMA), were synthesized by the RAFT process using ACVA as the initiator and CTP as the chain transfer agent. The glycopolymers prepared were subsequently characterized with ^{1}H NMR and GPC techniques (see Supporting Information, Figures S1 and S2 and Table S1). This was achieved first by polymerizing glycidyl methacrylate with GAEMA or LAEMA, followed by decoration of GMA surface with oligoamines to yield cationic copolymers $P(GMA\text{-}EDA)_7\text{-}st\text{-}P(GAEMA)_{22}$ and $P(GMA\text{-}EDA)_8\text{-}st\text{-}P(LAEMA)_{24}$ with molar masses of about 20 and 22 kDa, respectively, with narrow molecular weight distributions (M_w/M_n < 1.33) (see Supporting Information, Table S1 and Figure S1). It should be noted that the terminal dithioester RAFT group was reduced to free thiol by aminolysis during the amine decoration (Scheme 1).[45]

The successful formation of $P(GMA\text{-}EDA_7\text{-}st\text{-}GAEMA_{22})$ and $P(GMA\text{-}EDA_8\text{-}st\text{-}LAEMA_{24})$ was followed by ^{1}H NMR spectrum (Figure S2a,b) through the disappearances of the space isomerization of the epoxy group at 4.21 ppm (Figure S2a).[45] This was crucial since it reduces acute toxicity caused by degree of hydrolysis of macro chain transfer agent (CTAs), owing to free thioether end groups in living tissues interacting with a variety of proteins.[54] The free thiols also provide an accessible route for further functionalization of polymeric gold nanoparticles. The cationic polymers were further functionalized with dithiocarbamate by adding a slight excess of dithiocarbamate to the polymer at 0 °C and were characterized by^{1}H NMR and FTIR spectroscopy (see the Supporting Information, Figures S2c and S3).

The FTIR spectrum showed a characteristic C−S, C═S, and N−C signals at 987, 1050, and 1463 cm^{-1} for $P(GMA\text{-}EDAdtc)_7\text{-}st\text{-}P(GAEMA)_{22}$, respectively, while 987, 1050, and 1453 cm^{-1} were also recorded for $P(GMA\text{-}EDAdtc)_8\text{-}st\text{-}P(LAEMA)_{24}$ (Figure S3). The average hydrodynamic diameter of dithiocarbamate polymers in 150 mM PBS was determined by dynamic light scattering (DLS). Average sizes of 27.0 and 44.7 nm with moderate PDI (~0.30) were recorded (Table 1). The moderate PDI is ascribed to some aggregation of the polymers in aqueous solution. Polymeric dithiocarbamate derived from LAEMA and GAEMA was slightly negatively

Table 1. Average Hydrodynamic Diameter, PDI, Charge Distribution, and Zeta Potential of Dithiocarbamate Polymers in 150 mM PBS Solution

polymer	size (nm)	PDI	zeta potential
$p(GMA\text{-}EDAdtc)_8\text{-}st\text{-}p(LAEMA)_{24}$ (LPdtc)	44.7 ± 0.7	0.32	−10.13
$p(GMA\text{-}EDAdtc)_7\text{-}st\text{-}p(GAEMA)_{22}$ (GPdtc)	27.0 ± 0.8	0.34	−5.00

dx.doi.org/10.1021/bm5010977 | Biomacromolecules 2014, 15, 3802−3810

Scheme 2. Synthesis of Polymer Functionalized Gold Nanoparticles and Their Conjugation to the Anticancer Drug, Au(1)PPh_3

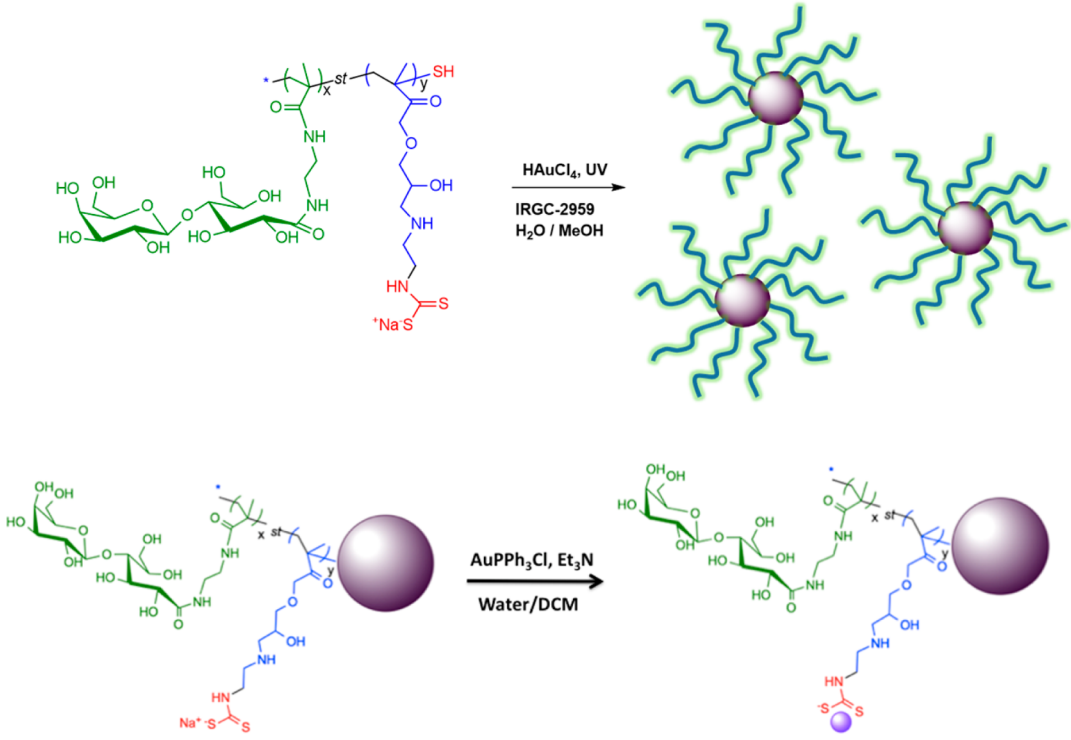

Table 2. DLS and TEM Data Showing the Effect of Polymeric Galactose Dithiocarbamate Concentration on GNPs Particle Size and Size Distribution Using a Molar Ratio of [$AuCl_4$]/[I] (1:3)

polymer	GNP code	polymer conc. (mg/mL)	TEM size (nm)	DLS size (nm)	PDI (size distri.)	zeta potential
LPdtc	**GNP-1**	1.0	40.2 ± 10.3	86.0 ± 1.1	0.27	−21.0
	GNP-2	2.0	16.7 ± 2.2	78.9 ± 9.0	0.25	−16.9
	GNP-3	5.0	13.3 ± 3.1	76.6 ± 1.6	0.20	−16.2
GPdtc	**GNP-4**	1.0	45.8 ± 12.7	110.7 ± 1.0	0.20	−13.3
	GNP-5	2.0	12.8 ± 4.2	60.1 ± 1.0	0.28	−10.5
	GNP-6	5.0	12.5 ± 3.7	31.3 ± 0.5	0.20	−10.3

charged, suggesting that all free amines in the polymers are functionalized with a dithiocarbamate motif. The glycopolymer segment is expected to impart biocompatibility and mediates the cellular interactions with nanoparticles, while the dithiocarbamate and the thiol moieties provide the functionality for gold nanoparticles stabilization and complexation with the gold(I) triphenyl phosphine on the surfaces of nanoparticles, respectively.

Synthesis of Statistical Glycopolymer Decorated Gold Nanoparticles. The preparation of glycopolymer functionalized gold nanoparticles was achieved via photoirradiation using Irgacure 2959 as photoinitiator (Scheme 2)[55−57] and was confirmed by transmission electron microscopy (TEM), UV−vis spectroscopy, and DLS analysis. The synthesized gold nanoparticles are expected to be stabilized by the dithiocarbamate pendant groups of the polymer, and therefore, they were expected to be more stable than thiol-stabilized gold nanoparticles due to the oxidative instability of the latter in physiological conditions.[58] In addition, the sulfur atoms of dithiocarbamate ligands possess *o*-donor and *n*-back-donation characteristics of the same order of magnitude. However, this moiety has a special attribute: there is an extra *n*-electron flow from nitrogen to sulfur via a planar delocalized π-orbital system, which results in strong electron donation and, hence, a high electron density on the metal leading to its stronger bond formation.[59] Two main forms of GNPs were synthesized from the statistical copolymers of p(GMA-EDAdtc)-st-p(LAEMA) (**GNP 1−3**) and p(GMA-EDAdtc)-st-p(GAEMA) (**GNP 4−6**). The gold nanoparticles were synthesized using varying concentrations of polymers in an effort to achieve near-monodisperse glyconanoparticles.

The visible absorption spectra of the glyconanoparticles aqueous solutions present a well-defined absorption band with a maximum at the wavelength λ_{max} = 526−538 nm and 536−550 nm for (**GNP 1−3**) and **GNP 4−6**, respectively (see Supporting Information, Figure S4). Typical results of hydrodynamic diameter measured by DLS showed different size GNPs, which can be found in the Supporting Information (Table 2). The results revealed that a range of AuNPs were successfully prepared having well-defined number-average particle sizes greater than 31.3 ± 0.5 nm (Table 2). The polydispersity index (PDI) of the particle size distributions as measured by DLS for all the GNPs ranged between 0.17 and 0.28, signifying a narrow particle size distribution. This observation was further supported by TEM micrographs of typical GNPs prepared in this study (Figure 1). Well monodispersed and smaller size spherical GNPs were formed with an increase in polymer concentration. The average size

dx.doi.org/10.1021/bm5010977 | *Biomacromolecules* 2014, 15, 3802−3810

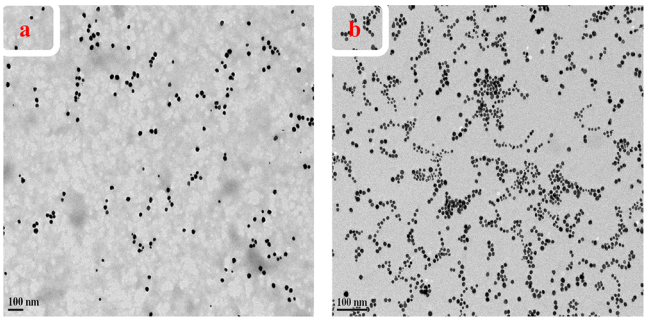

Figure 1. Representative TEM micrograph of (a) **GNP-3** and (b) **GNP-6**.

and particle size distribution of **GNPs 1−6** were also determined for each sample via TEM image from the diameter of at least 100 particles. The calculated size via TEM revealed particle sizes ranged between 12.5 ± 3.7−45.8 ± 12.7 nm (Table 2). The results obtained by both TEM and DLS indicate that the optimization of polymer concentration in solution is crucial to yield monodisperse nanoparticles of about 13 nm in diameter, as shown in Figure 1 and Table 2.

The stability of glycodithiocarbamate polymer modified gold nanoparticles was assessed by the dispersion of nanoparticles in high salt and pH conditions. Figure 2 below indicates that **GNP 1−6** are stable in physiological conditions, as no shift of the UV−vis peak was observed before and after their suspension in 10% NaCl solution, even after 1 week at normal temperature (Figure 2a). The gold nanoparticles were also found to be reasonably stable at physiological pH, as a bathochromic shift of ∼3 nm was observed at pH values between 6 and 8, with no broadening of surface plasmon resonance (SPR) band (Figure 2b).

Synthesis of Glyco-Decorated Gold Nanoparticles Functionalized Gold-Triphenyl Phosphine. Well-defined glyco-decorated gold nanoparticles gold(I) conjugates were prepared using glucose-derived and galactose-decorated dithiocarbamate-stabilized gold nanoparticles of about 13 nm in size and gold(I) triphenylphosphine chloride in a biphasic medium via a previously reported method (Figure 3).[20]

The successful conjugation of gold(I) was followed by TEM, UV−visible spectroscopy, DLS and by physical appearance. The UV−vis spectra showed a red shift of absorption band after the conjugation of gold(I) onto the surface of polymeric galactose gold nanoparticles (see Supporting Information, Figures S5 and S6). The red shifts of absorption band suggest an aggregation of GNP-$AuPPh_3$, which is also confirmed by TEM (Figure 4). For instance, **GNP-3** with a size of about 13 nm (Figure 1b) increased to about 21 nm after functionalization (Figure 4a, Table 3) via TEM calculation. This could be due to the hydrophobic nature of the gold(I) triphenylphosphine after conjugation to the GNPs. This was also evidenced by the change of color from red to purple (Figure 3) after conjugation. DLS data also confirmed the aggregation and an increase in polydispersity index (PDI; Table 3). It should be noted that TEM images show glyconanoparticles of smaller sizes, as compared to DLS. DLS measures the hydrodynamic radius of glyconanoparticles in solution, while glyconanoparticles are in dried state for TEM.[34] Therefore, even small traces of agglomerates can skew the DLS.[60] In addition, the TEM shows more clearly the core of nanoparticles (higher contrast of the gold core), while DLS takes the ligand shell into consideration, which may account for the difference in diameter of these glyconanoparticles.[61]

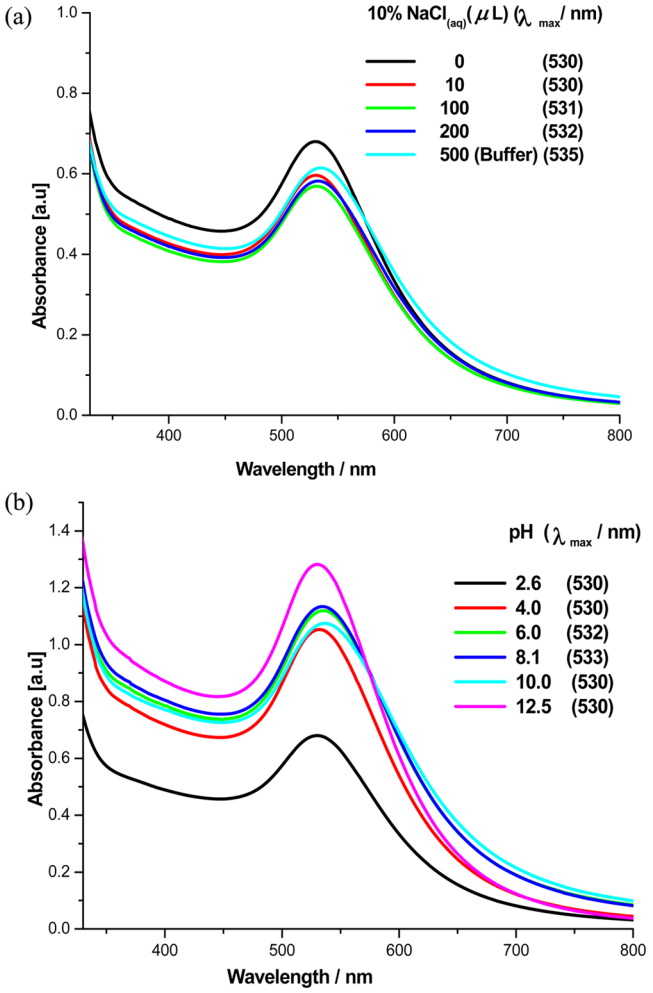

Figure 2. Representative UV−vis spectra of (a) gold nanoparticles after their dispersion in high salt solution of 10% NaCl and (b) gold nanoparticles at various pH using **GNP-3**.

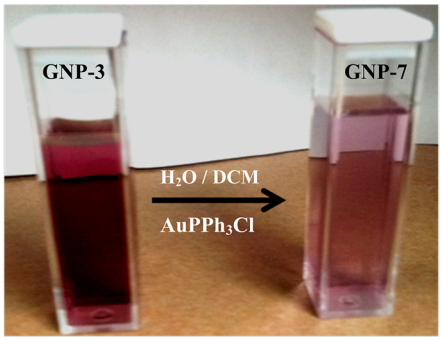

Figure 3. Representative image of galactose dithiocarbamate coated gold nanoparticles gold(I) conjugates **GNP-3** and **GNP-7**.

Cytotoxicity of Galactose-Decorated Gold Nanoparticles Functionalized Gold-Triphenyl Phosphine in Various Cell Lines. These glyconanoparticles and their gold(I) conjugates were studied for their cellular uptake and toxicity profiles in different cell lines. A cytotoxicity evaluation of gold(I) phosphine-based complexes using DTC ligands in selected cancer cell lines has been reported.[20,62−65] In general, it was found that **GNP-7**, [P(GMA-EDAdtc(Au(I)PPh_3)-st-

dx.doi.org/10.1021/bm5010977 | Biomacromolecules 2014, 15, 3802−3810

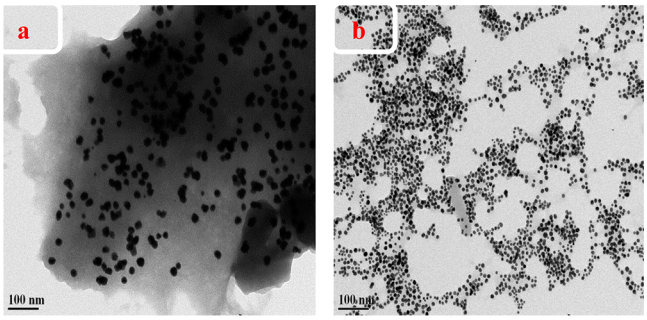

Figure 4. Representative TEM micrograph of (a) P(GMA-EDAdtc-(Au(I)PPh_3)-st-LAEMA)]AuNP (**GNP-7**) and (b) P(GMA-EDAdtc-(Au(I)PPh_3)-st-GAEMA)]AuNP (**GNP-8**).

Table 3. DLS and TEM Data Showing the Size and PDI of Au(I) Conjugate Gold Nanoparticles

phosphinogold(I)-AuNP conjugate	TEM size (nm)	DLS size (nm)	PDI (size distri.)	λ_{max} (nm)
GNP3-AuPPh$_3$ (GNP-7)	21.4 ± 2.9	246.6 ± 20	0.30	543
GNP6-AuPPh$_3$ (GNP-8)	14.1 ± 1.6	149.2 ± 4.4	0.38	538

LAEMA)]AuNP, showed the highest cytotoxicity toward HepG2 cells (IC_{50} = 4.13 ± 0.73 μg/mL) and was significantly more effective at inducing apoptosis and inhibiting cellular proliferation compared to well-known anticancer chemotherapeutics, such as cisplatin and cytarabine (IC_{50} = 30.11 and 320.07 μg/mL in HepG2, respectively; Table 4). Interestingly, **GNP-7** also showed approximately 2-fold higher cytotoxicity compared to its open-sugar derivative **GNP-8** in HepG2 cells (IC_{50} = 10.62 ± 1.31 μg/mL). This suggests the increase in toxicity may be attributed to the higher uptake of the galactose-based nanoparticles, which is believed to interact with the ASGPR, a lectin that has been well-characterized to be overexpressed on the cell surface in hepatocellular carcinomas and binds to galactose/asialoglycoprotein derivatives for endocytosis and delivery of biomaterials into the cell.[22,23] When compared with HeLa cells that are well-documented to be ASGPR deficient, a 4-fold decrease in toxicity (IC_{50} = 16.82 ± 0.51 μg/mL) was noted as compared to the HepG2 cell line.[66] Furthermore, MCF-7 cells have been reported to have lower levels of ASGPR expression in multiple studies, and cytotoxicity results with **GNP-7** demonstrated a 2.5-fold decrease in toxicity (IC_{50} = 11.39 ± 0.41 μg/mL) compared to the HepG2 cell line.[67−70] Other experiments with the open sugar derivative, **GNP-8**, showed similar toxicities in both the MCF7 and HepG2 cell lines, which indicates the specificity of ASGPR for galactose binding. These studies demonstrate **GNP-7** compound possess the highest selective toxicity toward HepG2 cells and therefore could be an effective system in targeted drug delivery by exploiting the ASGPR receptor. Similarly, the free polymeric glyconanoparticles **GNP-3** and **GNP-6** also showed good toxicity (IC_{50} = 15.34−17.65 μg/mL) against MCF7 (Table 4). This may be attributed to the architecture of the polymers on the GNPs surface, for example, the presence of DTC motif could enhance toxicity profile.[47,62−65]

Competition Binding Assay of ASGPR on Cell Surface with Asialofetuinand p(GMA-EDAdtc-st-LAEMA). Competitive binding assays were done to determine the role of inhibiting ASGPR by saturating the receptor with asialofetuin to prevent endocytosis of the galactose-decorated compound. Asialofetuin has been characterized as a native glycoprotein binding partner with the ASGPR.[53] In this study, when 10 μg/mL of **GNP-7** was incubated with HepG2 cells for 24 h, only 21.13 ± 2.61% of cells remained viable (Figure 5). However, the simultaneous incubation of asialofetuin at 10× the concentration (100 μg/mL) **GNP-7** showed reduced killing, resulting in 45.94 ± 8.31% viability. Interestingly, other experiments conducted by pretreating the cells with asialofetuin

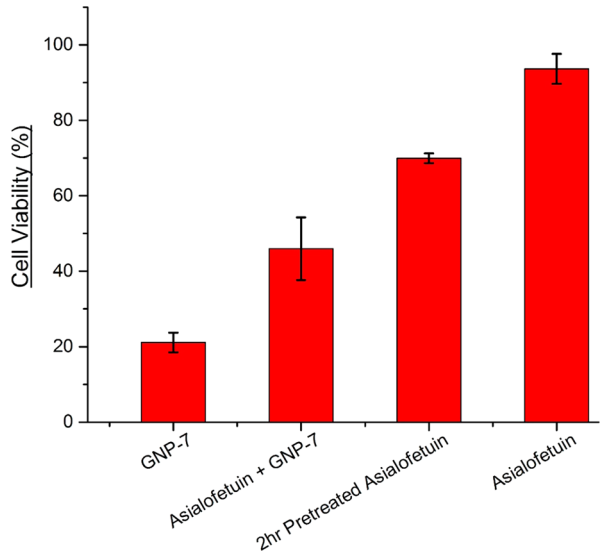

Figure 5. Competition binding assay between Asialofetuin and **GNP-7** in HepG2 cells over 24 h. Cells were treated with asialofetuin at 10× concentration of **GNP-7**.

Table 4. Inhibitory Concentration 50 (IC_{50}) of Glycopolymer-AuNP and Glycopolymer (Au(I)PPh_3)AuNP Derivatives in Cell Lines

		IC_{50} (μg/mL)			
compounds	compositions	MCF7 mammary adenocarcinoma	HepG2 hepatocellular carcinoma	Wi38 fibroblast	HeLa cervical carcinoma
cisplatin	cisplatin	20	30	30	
cytarabine	cytarabine	510	320	290	
GNP-3	[P(GMA-EDAdtc-st-LAEMA)]AuNP	17.65 ± 0.78	39.32 ± 3.12	56.20 ± 6.55	
GNP-6	[P(GMA-EDAdtc-st-GAEMA)]AuNP	15.34 ± 1.74	39.24 ± 2.67	55.83 ± 3.94	
GNP-7	[P(GMA-EDAdtc(Au(I)PPh_3)-st-LAEMA)] AuNP	11.39 ± 0.41	4.13 ± 0.73	13.42 ± 1.55	16.82 ± 0.51
GNP-8	[P(GMA-EDAdtc(Au(I)PPh_3)-st-GAEMA)] AuNP	9.63 ± 0.82	10.62 ± 1.31	17.16 ± 1.61	

dx.doi.org/10.1021/bm5010977 | *Biomacromolecules* 2014, 15, 3802−3810

at the same concentration for 2 h before the addition of **GNP-7** showed even more profound effects, with 69.95 ± 13.03% of cells viability. These studies indicate that the presence of asialofetuin may function to block the ASGPR receptor from interacting with the galactose constituent on **GNP-7**, thus, reducing efficiency of uptake and reduced cytotoxicity of the anticancer compound. Furthermore, these studies indicate that pretreatment of cells with asialofetuin for 2 h may bind to the ASGPR receptor causing internalization and reduced exposure on the cell surface, thus further reducing the cytotoxicity of the galactose-decorated AuNP.

A competitive binding study was then conducted with p(GMA-EDAdtc-st-LAEMA) polymer and its drug conjugated AuNP derivative, **GNP-7**. In this study, HepG2 and MCF7 were incubated with **GNP-7** at 10 and 17.5 μg/mL, respectively, and the cell viabilities were assessed at 24 h (Figure 6). While the unmodified P(GMA-EDAdtc-st-LAEMA)

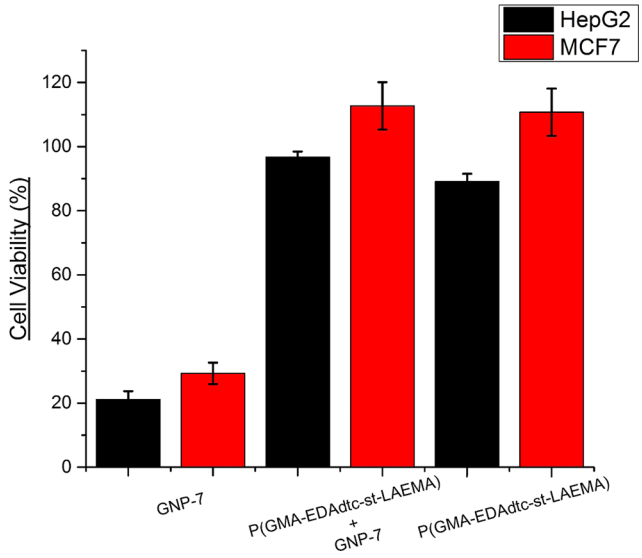

Figure 6. Competition binding assay between p(GMA-EDAdtc-st-LAEMA) polymer and **GNP-7** in HepG2 and MCF7 cell after 24 h.

polymer constituent was relatively nontoxic to the cells, the simultaneous incubation of p(GMA-EDAdtc-st-LAEMA) at 10× the concentration of **GNP-7** showed increased HepG2 and MCF7 cell viability and survivability, similar to the results in the asialofetuin competition binding assay (Figure 5). The ASGPR on the cell surface preferentially binds galactose and asialoglycprotein analogues. These results suggest that the galactose pendant groups on the glycopolymers may be binding to the ASGPR receptor and inhibiting the binding of the drug conjugated **GNP-7**. Alternatively, the binding of glycopolymer chains to the tumor cell surface may sterically hinder adjacent receptors from binding drug conjugated **GNP-7**. These studies further indicate that p(GMA-EDAdtc-st-LAEMA) is relatively nontoxic in solution with cytotoxicity similar to asialofetuin, a native glycoprotein ligand for the ASGPR (Figure 5).

CONCLUSION

We have successfully synthesized statistical glycopolymers decorated with dithiocarbamate via the RAFT polymerization. Subsequently, [glycopolymer-DTC] AuNPs and their Au(I)-PPh3 conjugates were synthesized and characterized in this comprehensive study. Here, we have shown the potential of a novel cancer therapeutic drug using glyconanoparticles conjugates for targeted delivery to ASGPR overexpressing HepG2 cells. The cytotoxic evaluation of the statistical glycopolymer-drug conjugated AuNPs showed that **GNP-7** had approximately 4-times higher cytotoxicity toward HepG2 cells overexpressing ASGPR as compared to ASGPR-deficient Hela cells. Therefore, the facile method of engineering glycopolymer-AuNP functionalized with anticancer agents may have interesting applications as versatile nanocarriers for targeted drug delivery systems in cancer therapy.

ASSOCIATED CONTENT

Supporting Information

^{1}H NMR, UV−vis spectra, and other characterization details. This material is available free of charge via the Internet at http://pubs.acs.org.

AUTHOR INFORMATION

Corresponding Author

*E-mail: narain@ualberta.ca. Phone: 1 780 492 1736.

Notes

The authors declare no competing financial interest.

ACKNOWLEDGMENTS

The authors would like to thank the Natural Sciences and Engineering Research Council of Canada (NSERC) and Alberta Innovates Health Solutions CRIO Program Award (PK#201201164) for generous funding of this research. Ms. Kate Agopsowicz is also thanked for her support and assistance with the cell culture.

REFERENCES

(1) Kelland, L. *Nat. Rev. Cancer* **2007**, *7*, 573−584.
(2) Boulikas, T.; Vougiouka, M. *Oncol. Rep.* **2003**, *10*, 1663−1682.
(3) Rieter, W. J.; Pott, K. M.; Taylor, K. M. L.; Lin, W. *J. Am. Chem. Soc.* **2008**, *130*, 11584−11585.
(4) Zutphen, S. V.; Reedijk, J. *Coord. Chem. Rev.* **2005**, *249*, 2845−2853.
(5) Florea, A.-M.; Büsselberg, D. *Cancers* **2011**, *3*, 1351−1371.
(6) Gottlieb, N. L.; Smith, P. M.; Smith, E. M. *Arthritis Rheum.* **1972**, *15*, 16−22.
(7) Cao-Milán, R.; Liz-Marzán, L. M. *Expert Opin. Drug Delivery* **2014**, *11*, 741−752.
(8) Jenkins, J. T.; Halaney, D. L.; Sokolov, K. V.; Ma, L. L.; Shipley, H. J.; Mahajan, S.; Louden, C. L.; Asmis, R.; Milner, T. E.; Johnston, K. P.; Feldman, M. D. *Nanomedicine (N. Y., NY, U. S.)* **2013**, *9*, 356−365.
(9) Huynh, V. T.; Chen, G.; Souza, P.; Stenzel, M. H. *Biomacromolecules* **2011**, *12*, 1738−1751.
(10) Huynh, V. T.; Quek, J. Y.; De Souza, P.; Stenzel, M. H. *Biomacromolecules* **2012**, *13*, 1010−1023.
(11) Allen, T. M. *Nat. Rev. Cancer* **2002**, 750.
(12) Huynh, V. T.; De Souza, P.; Stenzel, M. H. *Macromolecules* **2011**, *44*, 7888.
(13) Halimehjani, A. Z.; Marjani, K.; Ashouri, A. *Green Chem.* **2010**, *12*, 1306. (b) Wei, H.; Schellinger, J. G.; Chu, D. S. H.; Pun, S. H. *J. Am. Chem. Soc.* **2012**, *134*, 16554.
(14) Ahmed, M.; Wattanaarsakit, P.; Narain, R. *Eur. Polym. J.* **2013**, *49*, 3010−3033.
(15) Ahmed, M.; Narain, R. *Chem. Bioconjugates: Appl. Bioconjugates* **2013**, 444.
(16) Parry, A. L.; Clemson, A. N.; Ellis, J.; Bernhard, S. S. R.; Davis, B. G.; Cameron, N. R. *J. Am. Chem. Soc.* **2013**, *135*, 9362−9365.
(17) Narain, R. *Chemistry of Bioconjugates: Synthesis, Characterization, and Biomedical Applications*; John Wiley & Sons: New York, 2013.

(18) Takara, M.; Toyoshima, M.; Seto, H.; Hoshinoa, Y.; Miura, Y. *Polym. Chem.* **2014**, *5*, 931−939.
(19) Rossner, C.; Ebeling, B.; Vana, P. *ACS Macro Lett.* **2013**, *2*, 1073−1076.
(20) Ahmed, M.; Mamba, S.; Yang, X.-H.; Darkwa, J.; Kumar, P.; Narain, R. *Bioconjugate Chem.* **2013**, *24*, 979−986.
(21) Larsson, J.; Nolan, M.; Greer, J. *J. Phys. Chem. B* **2002**, *106*, 5931−5937.
(22) Yamazaki, N.; Kojima, S.; Bovin, N. V.; André, S.; Gabius, S.; Gabiusl, H.-J. *Adv. Drug Delivery Rev.* **2000**, *43*, 225−244.
(23) Cho, C. S.; Seo, S. J.; Park, I. K.; Kim, S. H.; Kim, T. H.; Hoshiba, T.; Harada, I.; Akaike, T. *Biomaterials* **2006**, *27*, 576−585.
(24) Li, Y.; Huang, G.; Diakur, J.; Wiebe, L. I. *Curr. Drug Delivery* **2008**, *5*, 299−302.
(25) Mi, F.-L.; Wu, Y.-Y.; Chiu, Y.-L.; Chen, M.-C.; Sung, H.-W.; Yu, S.-H.; Shyu, S.-S.; Huang, M.-F. *Biomacromolecules* **2007**, *8*, 892−898.
(26) Woodrow, K. A.; Bennett, K. M.; Lo, D. D. *Annu. Rev. Biomed. Eng.* **2012**, *14*, 17−46.
(27) Wilson-Welder, J. H.; Torres, M. P.; Kipper, M. J.; Mallapragada, S. K.; Wannemuehler, M. J.; Narasimhan, B. *J. Pharm. Sci.* **2009**, *98*, 1278−1316.
(28) Clark, M. A.; Jepson, M. A.; Hirst, B. H. *Adv. Drug Delivery Rev.* **2001**, *50*, 81−106.
(29) Huo, Q. *Colloids Surf., B* **2007**, *59*, 1−10.
(30) Ghosh, S. P.; Kim, C. K.; Han, G.; Forbes, S. N.; Rotello, M. V. *ACS Nano* **2008**, *2*, 2213−2218.
(31) Li, P.; Li, D.; Zhang, L.; Li, G.; Wang, E. *Biomaterials* **2008**, *29*, 3617−3624.
(32) Zhou, X.; Zhang, X.; Yu, X.; Zha, X.; Fu, Q.; Liu, B.; Wang, X.; Chen, Y.; Chen, Y.; Shan, Y.; Jin, Y.; Wu, Y.; Liu, J.; Kong, W.; Shen, J. *Biomaterials* **2008**, *29*, 111−117.
(33) Ahmed, M.; Narain, R. *Biomaterials* **2011**, *32*, 5279−5290.
(34) Ahmed, M.; Narain, R. *Biomaterials* **2012**, *33*, 3990−4001.
(35) Ahmed, M.; Deng, Z.; Liu, S.; Lafrenie, R.; Kumar, A.; Narain, R. *Bioconjugate Chem.* **2009**, *20*, 2169−2176.
(36) Ahmed, M.; Deng, Z.; Narain, R. *ACS Appl. Mater. Interfaces* **2009**, *1*, 1980−1987.
(37) Zheng, M.; Li, Z.; Huang, X. *Langmuir* **2004**, *20*, 4226−4235.
(38) Li, Z.-P.; Wang, Y.-C.; Liu, H.-C.; Li, Y.-K. *Anal. Chim. Acta* **2005**, *551*, 85−91.
(39) Shimmin, G. R.; Schoch, B. A.; Braun, V. P. *Langmuir* **2004**, *20*, 5613−5620.
(40) Guo, R.; Zhang, L.; Zhu, Z.; Jiang, X. *Langmuir* **2008**, *24*, 3459−3464.
(41) Das, j.; Huh, C.-H.; Kwon, K.; Park, S.; Jon, S.; Kim, K.; Yang, H. *Langmuir* **2009**, *25*, 235−241.
(42) Ahmed, M.; Narain, R. *Prog. Polym. Sci.* **2013**, *38*, 767.
(43) Chang, C. W.; Bays, E.; Tao, L.; Alconel, S. N. S.; Maynard, H. D. *Chem. Commun.* **2009**, *24*, 3580.
(44) Chu, D. S. H.; Schellinger, J. G.; Shi, J.; Convertine, A. J.; Stayton, P. S.; Pun, S. H. *Acc. Chem. Res.* **2012**, *45*, 1089.
(45) Wei, H.; Pahang, J. A.; Pun, S. H. *Biomacromolecules* **2013**, *14*, 275.
(46) Yang, X. C.; Chai, M. Y.; Zhu, Y.; Yang, W. T.; Xu, F. J. *Bioconjugate Chem.* **2012**, *23*, 618.
(47) Keter, F. K.; Guzei, I. A.; Nell, M.; van Zyl, W. E.; Darkwa, J. *Inorg. Chem.* **2014**, *53*, 2058−2067.
(48) Ahmed, M.; Jawanda, M.; Ishihara, K.; Narain, R. *Biomaterials* **2012**, *33*, 7858−7870.
(49) Ahmed, M.; Jiang, X.; Deng Z. Narain, R. *Bioconjugate Chem.* **2009**, *20*, 2017−2022.
(50) Deng, Z.; Li, S.; Jiang, X.; Narain, R. *Macromolecules* **2009**, *42*, 6393−6405.
(51) Narain, R.; Armes, S. P. *Chem. Commun.* **2002**, *23*, 2776−2777.
(52) Narain, R.; Armes, S. P. *Macromolecules* **2003**, *36*, 4675−4678.
(53) Narain, R.; Armes, S. P. *Biomacromolecules* **2003**, *4*, 1746−1758.
(54) Chang, C. W.; Bays, E.; Tao, L.; Alconel, S. N. S.; Maynard, H. D. *Chem. Commun.* **2009**, *24*, 3580−3582.
(55) Mcgilvray, L. K.; Decan, R. M.; Wang, D.; Scaiano, C. J. *J. Am. Chem. Soc.* **2006**, *128*, 15980−15981.
(56) Narain, R.; Housni, A.; Gody, G.; Boullanger, P.; Charreyre, M.; Delair, T. *Langmuir* **2008**, *23*, 12835−12841.
(57) Housni, A.; Ahmed, M.; Liu, S.; Narain, R. *J. Phys. Chem. C* **2008**, *112*, 12282−12290.
(58) Miyamoto, D.; Oishi, M.; Kojima, K.; Yoshimoto, K.; Nagasaki, Y. *Langmuir* **2008**, *24*, 5010−5017.
(59) Pandeya, K. B.; Singh, R.; Mathur, P. K.; Singh, R. P. *Transition Met. Chem.* **1986**, *11*, 340.
(60) Hall, J. B.; Dobrovolskaia, M. A.; Patri, A. K.; McNeil, S. E. *Nanomedicine* **2007**, *2*, 789−803.
(61) Housni, A.; Ahmed, M.; Liu, S.; Narain, R. *J. Phys. Chem. C* **2008**, *112*, 12282−12290.
(62) Tiekink, E. R. *Inflammopharmacology* **2008**, *16*, 138−142.
(63) Gracia-Orad, A.; Arizti, P.; Sommer, F.; Silvestro, L.; Massiot, P.; Chevallier, P.; Gutierrez-Zorilla, J. M.; Colacio, E.; De Pancorbo, M. M.; Tapiero, H. *Biomed. Pharmacother.* **1993**, *47*, 363−370.
(64) Nabipour, H.; Ghammamy, S.; Ashuri, S.; Aghbolagh, Z. S. *Org. Chem. J.* **2012**, *2*, 75−80.
(65) Nabipour, H.; Ghammamy, S.; Rahmani, A. *Micro Nano Lett.* **2011**, *6*, 217−220.
(66) KyungáKim, S.; MináPark, K.; JongáKim, W. *Chem. Commun.* **2010**, *46*, 692−694.
(67) Guo, R.; Yao, Y.; Cheng, G.; Wang, S. H.; Li, Y.; Shen, M.; Zhang, Y.; Baker, J. R.; Wang, J., Jr.; Shi, X. *RSC Adv.* **2012**, *2*, 99−102.
(68) Sanket, S.; Pankaj, P.; Ankitkumar, J.; Chandrashekhar, B.; Mangal, N. *Carbohydr. Res.* **2013**, *367*, 41−47.
(69) Medina, S.; Tekumalla, V.; Chevliakov, M.; Shewach, D.; Ensminger, W.; El-Sayed, M. *Biomaterials* **2011**, *32*, 4118−4129.
(70) Treichel, U.; Meyer zum Büschenfelde, K. H.; Dienes, H. P.; Gerken, G. *Arch. Virol.* **1997**, *142*, 493−498.